



ELSEVIER



CrossMark

journal homepage: [www.elsevier.com/locate/febsopenbio](http://www.elsevier.com/locate/febsopenbio)

## Small molecule antagonism of oxysterol-induced Epstein–Barr virus induced gene 2 (EBI2) activation<sup>☆</sup>

Tau Benned-Jensen<sup>a</sup>, Christian M. Madsen<sup>a</sup>, Kristine N. Arfelt<sup>a</sup>, Christian Smethurst<sup>b</sup>, Andy Blanchard<sup>b</sup>, Robert Jepras<sup>b</sup>, Mette M. Rosenkilde<sup>a,\*</sup>

<sup>a</sup>Laboratory for Molecular Pharmacology, Department of Neuroscience and Pharmacology, Faculty of Health and Medical Sciences, University of Copenhagen, Blegdamsvej 3, DK-2200 Copenhagen N, Denmark

<sup>b</sup>GlaxoSmithKline, Gunnels Wood Road, Stevenage SG1 2NY, United Kingdom

### ARTICLE INFO

#### Article history:

Received 11 February 2013

Received in revised form 14 February 2013

Accepted 14 February 2013

#### Keywords:

7TM receptors

EBI2

Oxysterols

Antagonism

MAP kinase activation

Epstein–Barr virus

### ABSTRACT

**The Epstein–Barr virus induced gene 2 (EBI2) was recently identified as the first oxysterol-activated 7TM receptor. EBI2 is essential for B cell trafficking within lymphoid tissues and thus the humoral immune response in general. Here we characterize the antagonism of the non-peptide molecule GSK682753A, which blocks oxysterol-induced G-protein activation,  $\beta$ -arrestin recruitment and B-cell chemotaxis. We furthermore demonstrate that activation triggers pertussis toxin-sensitive MAP kinase phosphorylation, which is also inhibited by GSK682753A. Thus, EBI2 signalling in B cells mediates key phenotypic functions via signalling pathways amenable to manipulation providing additional therapeutic options for inhibiting EBI2 activity.**

© 2013 The Authors. Published by Elsevier B.V. on behalf of Federation of European Biochemical Societies. All rights reserved.

### 1. Introduction

The Epstein–Barr virus induced gene 2 (EBI2 also known as GPR183) is a G protein-coupled seven-transmembrane (7TM) receptor that is predominantly expressed in B and T cells [1,2]. It regulates the trafficking of B cells within lymphoid tissues and is highly important for the generation of humoral immune responses [3,4]. EBI2 remained orphan for years; however, two independent studies recently showed that this receptor is activated by oxysterols, most potently by  $7\alpha,25$ -dihydroxycholesterol ( $7\alpha,25$ -OHC) [5,6]. Binding of oxysterols to EBI2 induce  $G\alpha_i$  activation,  $\beta$ -arrestin recruitment and ultimately migration of EBI2-expressing B and T cells. Thus, EBI2 functions as a chemo-attractant receptor. Interestingly, the main oxysterol generating cells within the lymphoid tissue were recently shown to be of stromal origin and these are required for efficient T cell-dependent plasma cell responses [7]. Moreover, we [8,9] and others [10] identified residues critical for oxysterol binding to EBI2 showing that the main anchor points are found in TM-II, -III, -VI and ECL2 of which

several are located in the minor binding pocket [11].

The expression of EBI2 has been found to be dysregulated in several types of B cell malignancies and is thus reduced in e.g. diffuse large B-cell lymphomas [12] and chronic lymphocytic leukemia [13] and increased in post-transplantation lymphoproliferative disorders (PTLDs) [14]. EBI2 is also highly expressed in EBV-transformed lymphoblastoid B cells which phenotypically resemble PTLDs [15]. We recently showed that increased expression of EBI2 potentiates antibody-induced proliferation in B cells [16]. Thus, in malignancies where EBI2 expression is increased, this receptor may contribute to pathogenesis possibly by potentiating B cell proliferation. In such cases, blocking EBI2 activity could serve as a target for pharmacotherapy. Furthermore, this could also be envisioned to apply in autoantibody-mediated diseases such as lupus and rheumatoid arthritis. Finally, the up-regulation of EBI2 upon EBV infection may function to position B cells in specific lymphoid zones in order to increase overall viral survival. Blocking EBI2 activity may therefore serve as a novel route to treat EBV infection as no EBV-specific drugs are currently available. Of note, EBI2 is expressed both in the latent and lytic infection stages as opposed to e.g. the EBV-encoded 7TM receptor BILF1 or other EBV genes [1,17]. The desire to develop tool compounds for modulating EBI2 activity is exemplified well by an ongoing uHTS screen at the Sanford-Burnham Center for Chemical Genomics where a range of compounds able to antagonize  $7\alpha,25$ -OHC-mediated  $\beta$ -arrestin recruitment has been identified in a primary screen (PubChem BioAssay ID: 651636).

<sup>☆</sup> This is an open-access article distributed under the terms of the Creative Commons Attribution-NonCommercial-No Derivative Works License, which permits non-commercial use, distribution, and reproduction in any medium, provided the original author and source are credited.

Abbreviations:  $7\alpha,25$ -OHC,  $7\alpha,25$ -dihydroxycholesterol; 7TM, seven-transmembrane; EBI2, Epstein–Barr virus induced gene 2; PTLD, post transplantation lymphoproliferative disorder; OE, over-expression; ptx, pertussis toxin.

\* Corresponding author. Tel.: +45 30604608; fax: +45 35327610.

E-mail address: [rosenkilde@sund.ku.dk](mailto:rosenkilde@sund.ku.dk) (M.M. Rosenkilde).

Simultaneous to the deorphanization of EBI2, we provided a characterization of a non-peptide inverse agonist (coined GSK682753A) that suppressed the apparent constitutive activity of the receptor [16]. Here we investigate the antagonistic properties of this compound and find that it potently suppresses  $7\alpha,25$ -OHC-mediated  $G\alpha_i$  activation,  $\beta$ -arrestin recruitment and chemotaxis of primary B cells *ex vivo*. Furthermore, for the first time we demonstrate that  $7\alpha,25$ -OHC-induced activation of EBI2 triggers pertussis toxin (ptx)-sensitive MAP kinase phosphorylation which also is suppressed by GSK682753A.

## 2. Materials and methods

### 2.1. Ligands

$7\alpha,25$ -OHC was purchased from Avanti Polar Lipids and GSK682753A was synthesized in-house at GlaxoSmithKline. Both were dissolved in DMSO; final DMSO concentration was 0.1%.

### 2.2. Transfection and cell culture

CHO cells were grown in RPMI1640 containing 10% FBS, 2 mM glutamine, 180 u/mL penicillin and 45  $\mu$ g/mL streptomycin (PenStrep) at 5%  $CO_2$  and 37 °C. Stably transfected CHO FLP-In cells were grown in the same medium also containing 600  $\mu$ g/mL Hygromycin. The CHO-K1 EA-arrestin cell line was grown in F-12 HAM medium containing 10% FBS, PenStrep and 250  $\mu$ g/mL Hygromycin.

### 2.3. Receptor constructs

All constructs contained an N-terminal M1-FLAG tag to facilitate immunostaining. This does not affect the ligand-induced activity of EBI2. Mutations were generated using the Quick Change protocol.

### 2.4. Membrane preparation

Membrane preparations of CHO FLP-In cells stably expressing M1-EBI2 wt or pcDNA5 were generated as previously described [9].

### 2.5. $GTP\gamma S$ binding assay

Measurement of  $GTP\gamma S$  binding to CHO FLP-In M1-EBI2 wt or pcDNA5 membranes upon  $7\alpha,25$ -OHC agonism or GSK682753A antagonism was performed as described previously [9]. Briefly, 10  $\mu$ g of membrane preparation was incubated 30 min in the presence of ligands at various concentrations and [ $^{35}S$ ]  $GTP\gamma S$  at 1 nM. Wheat-germ agglutinin-coupled SPA beads were subsequently added (2.8 mg/mL) followed by 30 min incubation. After centrifugation (1500 rpm, 5 min) the amount of  $GTP\gamma S$  binding was measured using a TopCounter. Unspecific binding was determined by adding unlabeled  $GTP\gamma S$  at 40  $\mu$ M.

### 2.6. $\beta$ -Arrestin recruitment

Recruitment of  $\beta$ -arrestin was measured using the PathHunter  $\beta$ -arrestin assay (DiscoverRx). cDNA encoding M1-EBI2 wt was fused to the PK1-tag and the small fragment of  $\beta$ -galactosidase and cloned into pcDNA3.1+. Assays were performed in a CHO-K1 EA-arrestin cell line stably expressing  $\beta$ -arrestin coupled to the  $\beta$ -gal large fragment. Cells were seeded out at 20,000 /well in 96-well plates and transfected the following day with 50 ng DNA using FuGENE6 reagent (0.15  $\mu$ L/well). 48 h after transfection, cells were stimulated with varying concentrations of  $7\alpha,25$ -OHC and/or GSK682753A for 90 min.  $\beta$ -Arrestin recruitment was detected as  $\beta$ -gal activity 60 min after addition of chemiluminescent substrate.

### 2.7. Chemotaxis

B cells were isolated from wt and EBI2-overexpressing C57BL/6 mice as previously described [16]. Chemotaxis was measured using 96-well ChemoTx plates with 5  $\mu$ m pores. Various concentrations of  $7\alpha,25$ -OHC and/or GSK682753A were applied to the lower chemotaxis chambers and 200,000 B cells subsequently added to the filter. The plates were incubated for 5 h at 37 °C and the number of cells migrated into the lower chambers detected using the CellTiterGlo dye and a TopCounter.

### 2.8. MAP kinase phosphorylation

CHO cells stably expressing EBI2 or pcDNA5 were seeded out in 12-well plates. The cells were serum starved overnight and incubated with GSK682753A and/or  $7\alpha,25$ -OHC at varying concentrations (for EBI2 and pcDNA) for 10 min. Subsequently, the cells were washed twice, lysed in lysis buffer (100 mM Tris, 4% SDS, 20% glycerol) and centrifuged for 5 min at 1500 rpm. 15–20  $\mu$ g protein was loaded on Bis-Tris 10% NuPAGE gels and run for 1.5 h at 140 V followed by blotting onto PVDF membranes for 1.5 h at 30 V. The membrane was blocked in TBST (1  $\times$  TBS with 0.1% Tween20) containing 5% BSA followed by incubation with rabbit anti-phospho ERK or anti-phospho p38 IgG antibody (1:1000). Following washing, the membrane was incubated in blocking buffer containing goat anti-rabbit-IgG HRP-conjugated antibody (1:10,000) and developed using Super-Signal West Pico substrate (Pierce). The amount of phosphorylation was measured using a FluorChem H2A camera. The membrane was subsequently stripped using Pierce stripping buffer (Pierce) and the procedure was then repeated with rabbit anti-ERK or anti-p38 IgG antibody to detect total ERK or p38 levels.

## 3. Results

### 3.1. GSK682753A antagonizes $7\alpha,25$ -OHC-induced EBI2 activation

GSK682753A is a piperidine-based non-peptide molecule identified in a compound library screen as an EBI2 inverse agonist [16] (Fig. 1A). To examine the putative antagonistic properties of GSK682753A we initially sought to determine whether GSK682753A was able to block oxysterol-induced activation of EBI2 at the level of G protein activation. In agreement with previous studies [5,6],  $7\alpha,25$ -OHC, the most potent EBI2-activating oxysterol, induced  $GTP\gamma S$  binding to membranes from CHO cells stably expressing EBI2 wt (but not to pcDNA5 controls) when present (Fig. 1B; [ $7\alpha,25$ -OHC] = 1 nM, [GSK682753A] = 0). However, presence of GSK682753A dose-dependently blocked EBI2 activity with an  $IC_{50}$  of 0.2  $\mu$ M demonstrating that GSK682753A indeed functions as an antagonist (Fig. 1B). To determine whether this antagonism is competitive or non-competitive, we investigated the effect of three different GSK682753A concentrations on  $7\alpha,25$ -OHC dose-response curves (Fig. 2A). As the presence of GSK682753A resulted in a right-ward shift in  $7\alpha,25$ -OHC potency curve with only limited effect on the efficacy, this suggest that GSK682753A functions as a competitive antagonist. This is further corroborated by Schild plot analysis showing a linear relationship between the concentration of GSK682753A and the  $\log(dr-1)$  value (Fig. 2B; slope: 1.4). The  $K_d$ , as estimated from the x-axis interception, is 64 nM.

To characterize the antagonism of GSK682753A further downstream and in a G protein-independent pathway, we measured  $\beta$ -arrestin recruitment in transiently transfected CHO cells.  $7\alpha,25$ -OHC induced  $\beta$ -arrestin recruitment with an  $EC_{50}$  value of 0.2  $\mu$ M in accordance with earlier studies [5,6] (Fig. 3A). GSK682753A also inhibited  $\beta$ -arrestin recruitment but with a slightly higher potency than in the  $GTP\gamma S$  binding assay ( $IC_{50}$  value of 40 nM; [ $7\alpha,25$ -OHC] = 1  $\mu$ M) (Fig. 3B). We have previously shown that the Phe at position

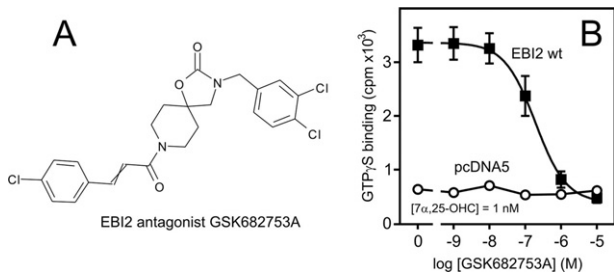


**Fig. 1.** (A) Chemical structure of GSK682753A. (B) Inhibition of [<sup>35</sup>S]GTP $\gamma$ S binding to membranes from CHO cells stably expressing FLAG-tagged human EB12 (solid squares) or pcDNA5 control (open circles) by GSK682753A in the presence of 1 nM 7 $\alpha$ ,25-OHC. The results are mean  $\pm$  SEM of raw data from three independent experiments.

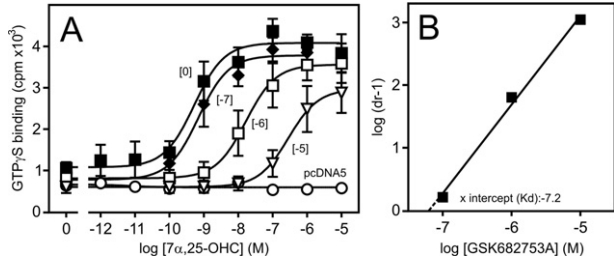


**Fig. 2.** (A) 7 $\alpha$ ,25-OHC-induced [<sup>35</sup>S]GTP $\gamma$ S binding to membranes from CHO cells stably expressing FLAG-tagged human EB12 or pcDNA5 (open circles) at various concentrations of GSK682753A: no antagonist ([0], solid squares), 100 nM ([−7], solid diamonds), 1  $\mu$ M ([−6], open squares) or 10  $\mu$ M ([−5], open triangles). The results are mean  $\pm$  SEM of raw data from three independent experiments. (B) Schild plot analysis of the dose–response curves presented in (A). The interception with the x-axis, which is an estimate of the log( $K_d$ ) value is given. The slope of the linear regression is 1.4.

III:08/3.32 in TM-III (F111) is crucial for the efficacy of GSK682753A as an inverse agonist [16]. To determine whether this also is the case for GSK682753A as an antagonist we mutated F111 to Ala and Tyr. Whereas F111 is not required for 7 $\alpha$ ,25-OHC binding (Fig. 3A) it is essential for the antagonism of GSK682753A as Ala but not Tyr substitution of F111 profoundly reduced the potency of GSK682753A (Fig. 3B).

Finally, as 7 $\alpha$ ,25-OHC functions as a chemoattractant [5,6], we examined whether GSK682753A is able to block 7 $\alpha$ ,25-OHC-induced chemotaxis of B cells *in vitro*. We used B cells from both wt and EB12-overexpressing (−OE) mice to assess the importance of EB12 expression level. 7 $\alpha$ ,25-OHC induced chemotaxis that peaked at 1 nM in both cases (Fig. 3C). EB12-OE cells tended to migrate more efficiently than their wt counterparts, which is in line with data from EB12-deficient and heterozygous B cells [5]. In agreement with the results from the GTP $\gamma$ S and  $\beta$ -arrestin recruitment assays, GSK682753A dose-dependently blocked the B cell migration (Fig. 3D; shown for EB12-OE cells only). Interestingly, the potency (7 pM) was much higher compared to the other assays. This could however be due to a generally higher sensitivity for ligand-modulation of EB12 in this assay as also the potency of the endogenous agonist 7 $\alpha$ ,25-OHC was increased. Thus, the EC<sub>50</sub> of the agonist was 0.1 nM in the chemotaxis assay compared to 1 and 100 nM the GTP $\gamma$ S (Fig. 2A) and  $\beta$ -arrestin recruitment (Fig. 3A) assays, respectively.

### 3.2. 7 $\alpha$ ,25-OHC induces MAP kinase activation

It has previously been shown that 7 $\alpha$ ,25-OHC activates the G $\alpha$ i pathway [5,6]. However, whether 7 $\alpha$ ,25-OHC induces MAP kinase activation upon binding to EB12 remains to be elucidated. To examine this, we measured ERK1/2 and p38 phosphorylation in CHO cells stably expressing EB12 in the presence of 7 $\alpha$ ,25-OHC. As seen in Fig. 4A, 7 $\alpha$ ,25-OHC induced a dose-dependent activation of ERK1/2 with a EC<sub>50</sub> value of 3 nM. This activation was inhibited by ptx indicating

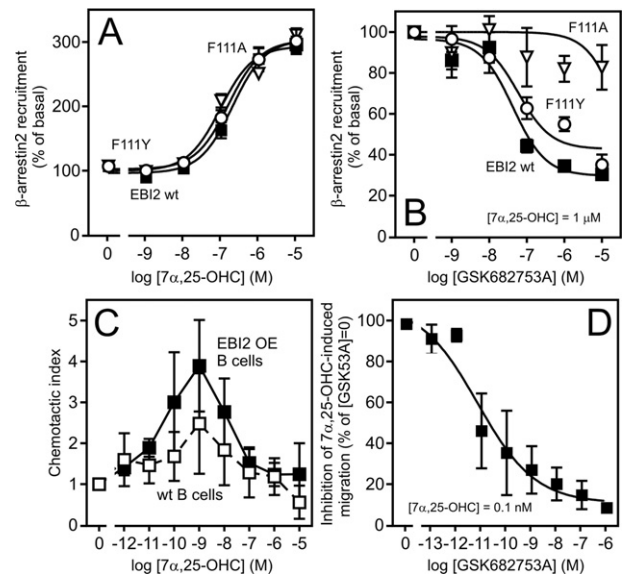


**Fig. 3.** (A) 7 $\alpha$ ,25-OHC-induced  $\beta$ -arrestin2 recruitment in CHO cells transiently transfected with FLAG- and PK1-tagged human EB12 wt (solid squares), F111Y mutant (open circles) or F111A mutant (open triangles). The results have been subtracted for background (pCMV transfected cells) and are given relative to the basal level, i.e. when no agonist is present, in percent as mean  $\pm$  SEM. The data are from at least three independent experiments. (B) Inhibition of  $\beta$ -arrestin2 recruitment in CHO cells transiently transfected with FLAG- and PK1-tagged human EB12 wt (solid squares), F111Y mutant (open circles) or F111A mutant (open triangles) by GSK682753A in the presence of 1  $\mu$ M 7 $\alpha$ ,25-OHC. The results have been subtracted for background (pCMV transfected cells) and are given relative to the basal level, i.e. when 1  $\mu$ M 7 $\alpha$ ,25-OHC but no antagonist is present, in percent as mean  $\pm$  SEM. The data are from at least three independent experiments. (C) *Ex vivo* chemotaxis of B cells isolated from wt (open squares) or EB12-overexpressing (solid squares) mice towards a gradient of 7 $\alpha$ ,25-OHC. The data are presented as chemotactic index as mean  $\pm$  SEM and are from four independent experiments. (D) Inhibition of chemotaxis of EB12-overexpressing B cells by GSK682753A in the presence of 0.1 nM 7 $\alpha$ ,25-OHC but no antagonist is present, in percent as mean  $\pm$  SEM. The data are from three independent experiments.

ERK1/2 phosphorylation to be dependent of G $\alpha$ i pathway activity. In line with this, GSK682753A also inhibited ERK1/2 activation with an IC<sub>50</sub> of 8 nM (Fig. 4B). Finally, we also examined whether EB12 activation results in activation of the p38 MAP kinase. As seen in Fig. 4C, like ERK, p38 was dose-dependently activated by 7 $\alpha$ ,25-OHC in a ptx-sensitive manner. Thus, oxysterol binding to EB12 leads to activation of at least two MAP kinases.

## 4. Discussion

Much has been learned about the biology and pharmacology of EB12 in the past 2 years. Thus, both the endogenous agonist [5,6], the cellular producers of this agonist [7] and the molecular pharmacology of 7 $\alpha$ ,25-OHC, the most potent agonist, [9,10] have all been characterized within this period. In addition, just prior to the deorphanization, we presented a non-peptide compound, GSK682753A, which inhibited the apparent constitutive activity of EB12 [16]. Here, we have investigated the antagonistic properties of this molecule showing that it blocks oxysterol-induced G protein activation (Figs. 1 and 2),  $\beta$ -arrestin recruitment (Fig. 3A and B), B cell chemotaxis (Fig. 3C and D) and ERK activation (Fig. 4). Compared to the *in vitro* assays, the potency measured in the *ex vivo* chemotaxis assay was much higher. At present we cannot explain this difference. However, we have recently characterized a series of CCR8 antagonists and also observed higher potencies in chemotaxis assays compared to IP<sub>3</sub> accumulation [18], and in line with the concomitant higher potency of 7 $\alpha$ ,25-OHC it is possible that an increase in assay sensitivity could be a contributing factor.

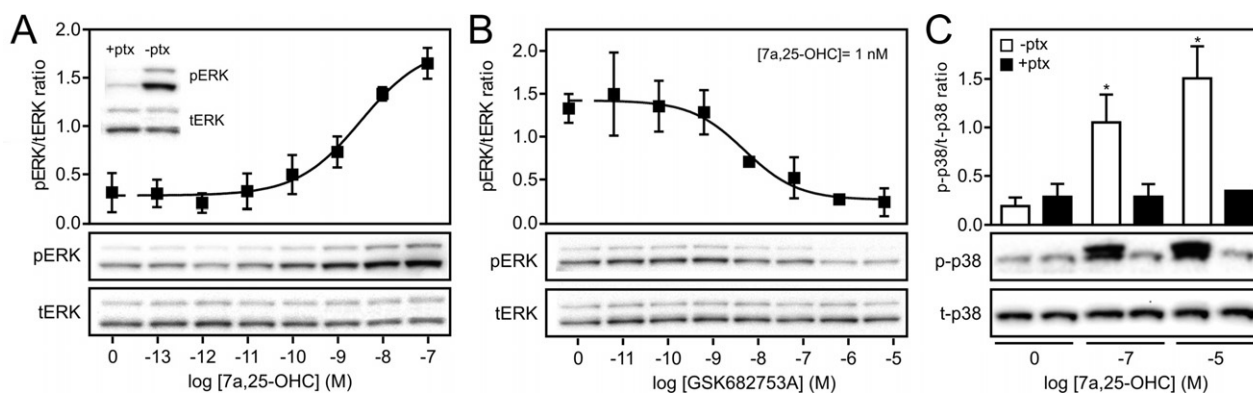


**Fig. 4.** (A)  $7\alpha,25$ -OHC-induced ERK activation in serum-starved CHO cells stably expressing FLAG-tagged human EB12. The data are presented as the ratio between phosphorylated ERK (pERK) and total ERK (tERK) as mean  $\pm$  SEM from three independent experiments. Representative blots of pERK and tERK are shown below. *Inset*, ERK phosphorylation by 100 nM  $7\alpha,25$ -OHC in cells incubated overnight with 100 ng/mL pertussis toxin (+ ptx) or DMSO vehicle (- ptx). (B) Inhibition of ERK activation by GSK682753A in the presence of 1 nM  $7\alpha,25$ -OHC. Presented as in (A). (C)  $7\alpha,25$ -OHC-induced p38 activation in serum-starved CHO cells stably expressing FLAG-tagged human EB12 in after overnight incubation with pertussis toxin (+ ptx, filled columns) or DMSO control (- ptx, empty columns). The data are presented as the ratio between phosphorylated p38 (p-p38) and total p38 (t-p38) as mean  $\pm$  SEM from three independent experiments. Representative blots of p-p38 and t-p38 are shown below. \* $p < 0.05$  by Student's *t*-test.

Collectively, our results indicate that GSK682753A functions as a competitive antagonist and binds to the receptor in the same region as  $7\alpha,25$ -OHC. First, we observe linearity in the Schild plot analysis (Fig. 2B). Second, GSK682753A is highly dependent on F111 at position III:08/3.32 in TM-III (Fig. 3B). Although this is not the case for  $7\alpha,25$ -OHC (Fig. 3A), it has recently been shown that the TM-III residues Y112 at position III:09/3.33 (just next to F111) and Y116 at III:13/3.37 are crucial for agonist binding [9,10] indicating that the two ligands bind in the same region. Interestingly, the primary uHTS screen at Sanford-Burnham Center for Chemical Genomics identified 2946 compounds out of 364,168 tested that were able to suppress  $7\alpha,25$ -OHC-induced  $\beta$ -arrestin recruitment at 5  $\mu$ M by more than 50% (PubChem BioAssay ID: 651636). Of note, the most efficacious of the active compounds are very similar in structure to GSK682753A. For instance, the best compound (CID: 5804570) also has two chlorine-substituted benzene-rings at each extremity, an enone moiety and a centrally-located nitrogen-containing ring (in this case a piperazine). Thus, it seems that these structural traits are important for efficacious inhibition of EB12 activity. It should be noted that we first characterized GSK682753A as an inverse agonist [16]. However, new data indicate that a part of the constitutive activity of EB12 may be a result of oxysterol contamination in the medium [9]. Thus, the inverse agonism of GSK682753A might have been antagonistic. It is possible that EB12 is constitutively active; however, presently we cannot assess the magnitude of this (if any) with the tools available.

As EB12 is highly important for generation of an efficient T cell-dependent humoral immune response [5–7] it may be that aberrant expression or other dysregulation of this receptor contributes in B cell pathologies. In line with this, EB12 expression is down-regulated in diffuse large B-cell lymphomas [12] and chronic lymphocytic leukemia [13] but up-regulated in PTLDs [14]. Interestingly, PTLDs are highly associated with Epstein–Barr virus (EBV) seropositivity which agrees well with the finding that EBV infection of B cells *in vitro* results in transformation of these into highly proliferative lymphoblastoids [19]. In both cases, the expression of EB12 is highly upregulated suggesting that this receptor could play a role in pathogenesis [2,15] putatively in combination with BILF1 [20]. This is also indicated by the observation that the proliferation of B cells over-expressing EB12 is higher than wt counterparts [16]. Importantly, the proliferation could be blocked by GSK682753A suggesting that targeting EB12 could be therapeutically beneficial. This may not only be limited to malignant diseases but may also extend to EBV-associated benign conditions such as mononucleosis for which no treatment is currently available.

## Funding

The work presented here was supported by financial grants from the NovoNordisk Foundation, The Danish Council for Independent Research | Medical Sciences, and the Aase and Einar Danielsen Foundation. None of the funding sources were involved in the present work.

## Acknowledgements

We thank Inger Smith Simonsen for excellent technical assistance.

## References

- [1] Rosenkilde M.M., Benned-Jensen T., Andersen H., Holst P.J., Kledal T.N., Luttichau H.R. et al. (2006) Molecular pharmacological phenotyping of EB12. An orphan seven-transmembrane receptor with constitutive activity. *J. Biol. Chem.* 281, 13199–13208.
- [2] Birkenbach M., Josefsen K., Yalamanchili R., Lenoir G., Kieff E. (1993) Epstein–Barr virus-induced genes: first lymphocyte-specific G protein-coupled peptide receptors. *J. Virol.* 67, 2209–2220.
- [3] Pereira J.P., Kelly L.M., Xu Y., Cyster J.G. (2009) EB12 mediates B cell segregation between the outer and centre follicle. *Nature* 460, 1122–1126.
- [4] Gatto D., Paus D., Basten A., Mackay C.R., Brink R. (2009) Guidance of B cells by the orphan G protein-coupled receptor EB12 shapes humoral immune responses. *Immunity* 31, 259–269.
- [5] Liu C., Yang X.V., Wu J., Kuei C., Mani N.S., Zhang L. et al. (2011) Oxysterols direct B-cell migration through EB12. *Nature* 475, 519–523.
- [6] Hannedouche S., Zhang J., Yi T., Shen W., Nguyen D., Pereira J.P. et al. (2011) Oxysterols direct immune cell migration via EB12. *Nature* 475, 524–527.
- [7] Yi T., Wang X., Kelly L.M., An J., Xu Y., Sailer A.W. et al. (2012) Oxysterol gradient generation by lymphoid stromal cells guides activated B cell movement during humoral responses. *Immunity* 37, 535–548.
- [8] Benned-Jensen T., Rosenkilde M.M. (2008) Structural motifs of importance for the constitutive activity of the orphan 7TM receptor EB12: analysis of receptor activation in the absence of an agonist. *Mol. Pharmacol.* 74, 1008–1021.
- [9] Benned-Jensen T., Norn C., Laurent S., Madsen C.M., Larsen H.M., Arfelt K.N. et al. (2012) Molecular characterization of oxysterol binding to the Epstein–Barr virus-induced gene 2 (GPR183). *J. Biol. Chem.* 287, 35470–35483.
- [10] Zhang L., Shih A.Y., Yang X.V., Kuei C., Wu J., Deng X. et al. (2012) Identification of structural motifs critical for EB12 function and homology modeling of ligand docking site. *Mol. Pharmacol.* 82, 1094–1103.
- [11] Rosenkilde M.M., Benned-Jensen T., Frimurer T.M., Schwartz T.W. (2010) The minor binding pocket: a major player in 7TM receptor activation. *Trends Pharmacol. Sci.* 31, 567–574.
- [12] Alizadeh A.A., Eisen M.B., Davis R.E., Ma C., Lossos I.S., Rosenwald A. et al. (2000) Distinct types of diffuse large B-cell lymphoma identified by gene expression profiling. *Nature* 403, 503–511.
- [13] Aalto Y., El-Rifa W., Vilpo L., Ollila J., Nagy B., Vihinen M. et al. (2001) Distinct gene expression profiling in chronic lymphocytic leukemia with 11q23 deletion. *Leukemia* 15, 1721–1728.
- [14] Craig F.E., Johnson L.R., Harvey S.A., Nalesnik M.A., Luo J.H., Bhattacharya S.D.

- et al. (2007) Gene expression profiling of Epstein–Barr virus-positive and -negative monomorphic B-cell posttransplant lymphoproliferative disorders. *Diagn. Mol. Pathol.* 16, 158–168.
- [15] Cahir-McFarland E.D., Carter K., Rosenwald A., Giltnane J.M., Henrickson S.E., Staudt L.M. et al. (2004) Role of NF-kappa B in cell survival and transcription of latent membrane protein 1-expressing or Epstein–Barr virus latency III-infected cells. *J. Virol.* 78, 4108–4119.
- [16] Benned-Jensen T., Smethurst C., Holst P.J., Page K.R., Sauls H., Sivertsen B. et al. (2011) Ligand modulation of the Epstein–Barr virus-induced seven-transmembrane receptor EB12: identification of a potent and efficacious inverse agonist. *J. Biol. Chem.* 286, 29292–29302.
- [17] Paulsen S.J., Rosenkilde M.M., Eugen-Olsen J., Kledal T.N. (2005) Epstein–Barr virus-encoded BILF1 is a constitutively active G protein-coupled receptor. *J. Virol.* 79, 536–546.
- [18] Rummel P., Arfelt K., Baumann L., Jenkins T., Thiele S., Luttichau H. et al. (2012) Molecular requirements for inhibition of the chemokine receptor CCR8 – probe-dependent allosteric interactions. *Br. J. Pharmacol.* 167, 1206–1217.
- [19] Young L.S., Rickinson A.B. (2004) Epstein–Barr virus: 40 years on. *Nat. Rev. Cancer* 4, 757–768.
- [20] Lyngaa R., Norregaard K., Kristensen M., Kubale V., Rosenkilde M.M., Kledal T.N. (2010) Cell transformation mediated by the Epstein–Barr virus G protein-coupled receptor BILF1 is dependent on constitutive signaling. *Oncogene* 29, 4388–4398.